

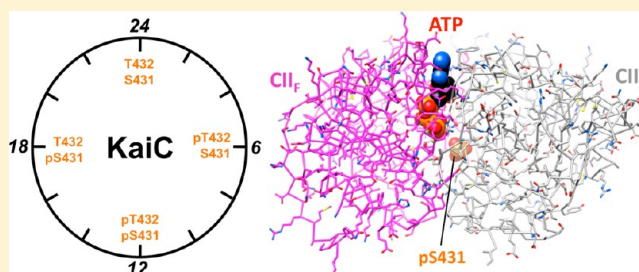
# Dephosphorylation of the Core Clock Protein KaiC in the Cyanobacterial KaiABC Circadian Oscillator Proceeds via an ATP Synthase Mechanism

Martin Egli,<sup>\*,†</sup> Tetsuya Mori,<sup>‡</sup> Rekha Pattanayek,<sup>†</sup> Yao Xu,<sup>‡</sup> Ximing Qin,<sup>‡</sup> and Carl H. Johnson<sup>‡</sup>

<sup>†</sup>Department of Biochemistry, Vanderbilt University, School of Medicine, Nashville, Tennessee 37232, United States

<sup>‡</sup>Department of Biological Sciences, College of Arts and Science, Vanderbilt University, Nashville, Tennessee 37235, United States

**ABSTRACT:** The circadian clock of the cyanobacterium *Synechococcus elongatus* can be reconstituted in vitro from three proteins, KaiA, KaiB, and KaiC in the presence of ATP, to tick in a temperature-compensated manner. KaiC, the central cog of this oscillator, forms a homo-hexamer with 12 ATP molecules bound between its N- and C-terminal domains and exhibits unusual properties. Both the N-terminal (CI) and C-terminal (CII) domains harbor ATPase activity, and the subunit interfaces between CII domains are the sites of autokinase and autophosphatase activities. Hydrolysis of ATP correlates with phosphorylation at threonine and serine sites across subunits in an orchestrated manner, such that first T432 and then S431 are phosphorylated, followed by dephosphorylation of these residues in the same order. Although structural work has provided insight into the mechanisms of ATPase and kinase, the location and mechanism of the phosphatase have remained enigmatic. From the available experimental data based on a range of approaches, including KaiC crystal structures and small-angle X-ray scattering models, metal ion dependence, site-directed mutagenesis (i.e., E318, the general base), and measurements of the associated clock periods, phosphorylation patterns, and dephosphorylation courses as well as a lack of sequence motifs in KaiC that are typically associated with known phosphatases, we hypothesized that KaiCII makes use of the same active site for phosphorylation and dephosphorylation. We observed that wild-type KaiC (wt-KaiC) exhibits an ATP synthase activity that is significantly reduced in the T432A/S431A mutant. We interpret the first observation as evidence that KaiCII is a phosphotransferase instead of a phosphatase and the second that the enzyme is capable of generating ATP, both from ADP and P<sub>i</sub> (in a reversal of the ATPase reaction) and from ADP and P-T432/P-S431 (dephosphorylation). This new concept regarding the mechanism of dephosphorylation is also supported by the strikingly similar makeups of the active sites at the interfaces between  $\alpha/\beta$  heterodimers of F<sub>1</sub>-ATPase and between monomeric subunits in the KaiCII hexamer. Several KaiCII residues play a critical role in the relative activities of kinase and ATP synthase, among them R385, which stabilizes the compact form and helps kinase action reach a plateau, and T426, a short-lived phosphorylation site that promotes and affects the order of dephosphorylation.



## ■ KAIABC CIRCADIAN CLOCK IN *SYNECHOCOCCUS ELONGATUS*

Circadian clocks are endogenous biological timers that rhythmically regulate numerous processes with a roughly 24 h period and exhibit temperature compensation.<sup>1</sup> Such clocks exist in a range of eukaryotic systems, including mammals, plants, fungi, and insects, and have also been found in cyanobacteria.<sup>2,3</sup> The latter are the simplest organisms known to possess a clock, and in the model organism *Synechococcus elongatus* PCC 7942 (*S. elongatus*), the *kaiA*, *kaiB*, and *kaiC* genes that form a cluster on the chromosome were shown to be essential for proper circadian function.<sup>4</sup> The observation that KaiA and KaiC proteins positively and negatively regulate *kaiBC* transcription, respectively,<sup>4</sup> initially rendered the cyanobacterial clock consistent with a transcription–translation oscillatory feedback loop (TTFL) model, believed to be at the core of all self-sustaining biological timers.<sup>1</sup>

The cyanobacterial clock continues to run in constant darkness and in the presence of translational inhibitors.<sup>5,6</sup> Moreover, translational inhibitors do not strongly reset the phase of the cyanobacterial clock.<sup>5</sup> Kondo and co-workers reported robust circadian rhythms under constant dark conditions in the presence of excess amounts of transcription inhibitors that almost quantitatively block RNA and protein synthesis;<sup>6</sup> these experiments with inhibitors and in darkness cast doubt on the need for a TTFL to sustain rhythms. Even more astonishing than the observation that the cyanobacterial circadian clock was able to function without de novo synthesis of clock gene mRNAs and the proteins encoded by them was the subsequent discovery that the clock can be reconstituted in vitro from the KaiA, KaiB, and KaiC proteins in the presence of

**Received:** September 30, 2011

**Revised:** January 6, 2012

**Published:** February 2, 2012

ATP.<sup>7</sup> This “test tube” clock not only ticks with a regular period of 24 h but also is temperature-compensated, and mutations in any of the three proteins trigger alterations in the period that resemble those of the corresponding mutant strains *in vivo*. There is good evidence that this KaiABC post-translational oscillator (PTO) represents the master timer and that it exerts control over the TTFL and clock-controlled gene expression.<sup>8,9</sup> These properties render the KaiABC clock an attractive target for detailed biochemical, biophysical, and structural investigations that are expected to furnish insights into the mechanistic underpinnings of a biological clockwork.

### ■ KAIC COMBINES ATPASE, AUTOKINASE, AND AUTOPHOSPHATASE ACTIVITIES

The KaiA, KaiB, and KaiC proteins interact with each other *in vitro* and *in vivo*,<sup>10–16</sup> and KaiC constitutes the central component of the protein complex.<sup>17</sup> KaiC is the result of a gene duplication (Figure 1A), and the two halves bear similarity to members of the *recA* gene family of ATP-dependent recombinases.<sup>18</sup> Besides exhibiting ATPase activity,<sup>19,20</sup> KaiC is also an autokinase and an autophosphatase *in vitro* and *in vivo*,<sup>21–23</sup> and clock speed is correlated with the level of phosphorylation.<sup>23</sup> Both *in vitro* and *in vivo*, KaiA enhances phosphorylation of KaiC and KaiB antagonizes the action of KaiA.<sup>22–25</sup> Binding of KaiB coincides with KaiC subunit exchange<sup>26</sup> that is important for maintaining a robust amplitude.<sup>27</sup>

The crystal structure of the full-length KaiC protein from *S. elongatus* revealed formation of a homohexamer in the shape of a double doughnut with a central pore and 12 ATP molecules bound between the interfaces of the subunits (Figure 1B).<sup>28</sup> The N-terminal ring and domain are termed CI, and the C-terminal ring and domain are termed CII. Residues T432 and S431 in the CII half were identified as phosphorylation sites by X-ray crystallography<sup>29</sup> and mass spectrometry.<sup>30</sup> These serine and threonine residues, when mutated to alanine individually, render the clock arrhythmic,<sup>29</sup> and KaiC can therefore be classified as a Ser/Thr kinase. None of the tyrosine residues were observed to carry a phosphate group, and the KaiCI half appears to be devoid of phosphorylation sites.

In the crystal structure, the hydroxyl group of T426 is hydrogen bonded to the phosphate of pS431, and we proposed that T426 constitutes a third phosphorylation site based on the arrhythmic phenotype of the T426A mutant.<sup>29</sup> Indeed, crystal structures of KaiC phosphorylation site mutant proteins, such as S431A and T432E/S431A, revealed phosphorylated T426 residues.<sup>31</sup> However, phosphorylation of T426 by mass spectrometric methods has not been reported to date, implying that the T426 phosphate group is highly labile or is perhaps disrupted by preparation of the protein for mass spectrometry. KaiC mutant strains such as T426E and T426N exhibited arrhythmic behavior,<sup>32</sup> demonstrating that T426 needs to be able to be phosphorylated and not just capable of forming a hydrogen bond to pS431 (as observed in the crystal structure of the KaiC T426N mutant).<sup>31</sup> Phosphorylation and dephosphorylation of the T432 and S431 residues follow a strict order, whereby T432 captures a phosphate before S431 and also becomes dephosphorylated first (TS → pTS → pTpS → TpS → TS).<sup>33,34</sup>

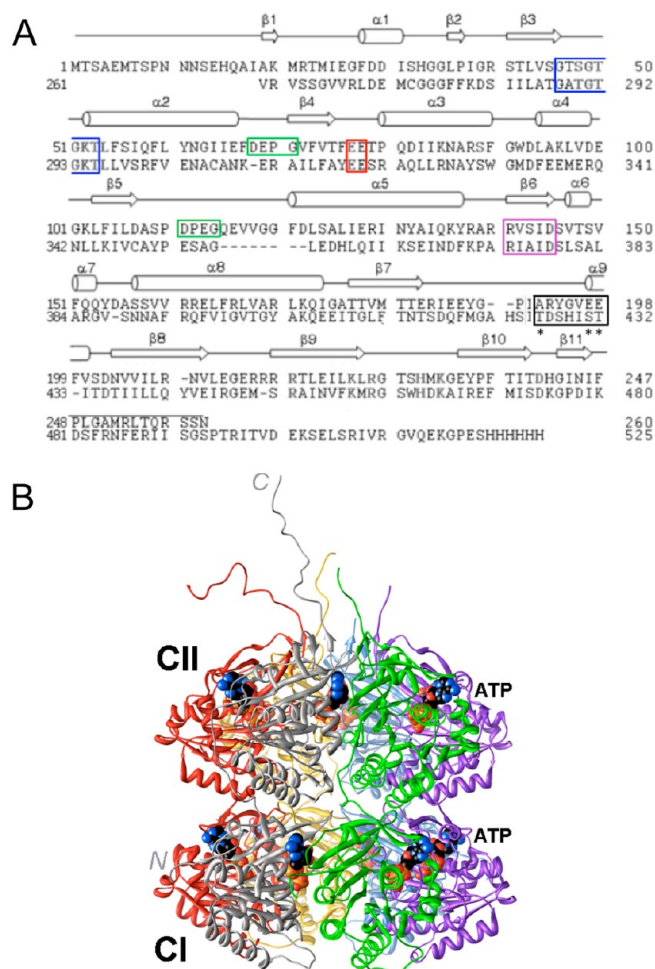


**Figure 1.** Amino acid sequence and three-dimensional structure of *S. elongatus* KaiC. (A) Sequence alignment of the N- and C-terminal halves of KaiC (CI on the top and CII on the bottom, respectively). Secondary structure elements as observed in the crystal structure<sup>28</sup> are denoted above the primary structure, and selected regions are boxed: Walker A motif (P-loop GXXXXGKT, blue), truncated Walker B motif (RXXXX, purple), sequence conserved in some GTP-binding proteins (DXXG, green), putative catalytic carboxylate(s) (red), and phosphorylation loop (black, phosphorylation sites in CII, T432, S431, and T426 marked with asterisks). (B) Crystal structure of full-length KaiC (Protein Data Bank entry 3DVL).<sup>12,28</sup> Hexamer subunits A–F are colored gray, green, magenta, blue, yellow, and red, respectively. ATP molecules bound between subunits are shown in space filling mode with carbon atoms colored black. At the N-terminal end of CI, residues 1–13 are missing. C-Terminal peptide tails of CII (residues 489–519) that serve as the binding site for KaiA<sup>12,49</sup> were only traced completely for subunits A and F.

### ■ CATALYTIC GLUTAMATES AND CI ATPASE AND CII KINASE

The ATP molecules bound between subunits are recognized differently in the CI and CII halves. In CI, the adenine nucleobase is contacted by amino acids under formation of three hydrogen bonds.<sup>28</sup> These interactions are absent in the CII half, and the stabilities of the CI and CII hexamers based on separately expressed domains differ.<sup>35</sup> Whereas CI domains hexamerize, no hexamer formation was observed for the CII domain in EM micrographs.<sup>14</sup> These differences in structure and stability go along with the functional specialization of the CI and CII rings. The former appears to serve as a structural

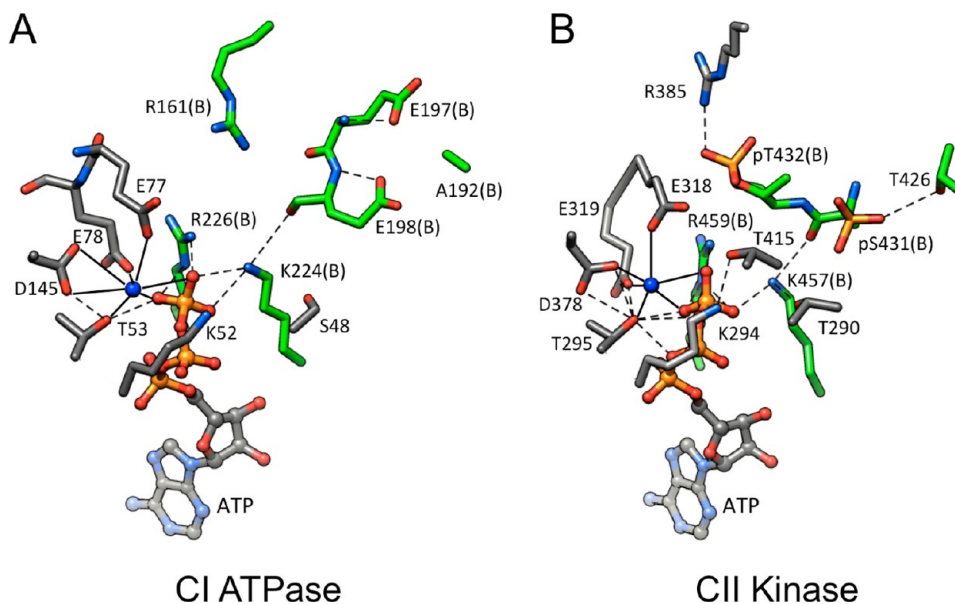


**Figure 2.** Intersubunit ATP binding sites in KaiC.<sup>31</sup> (A) ATPase active site in CI. (B) Kinase/ATPase active site in CII. Residues from subunits A and B are colored gray and green, respectively, matching the subunit coloring scheme in Figure 1B, and are labeled. The ligand spheres of Mg<sup>2+</sup> ions are denoted with solid lines, and hydrogen bonds are shown as dashed lines.

platform<sup>14,28</sup> and power generator,<sup>19</sup> and the latter harbors the phosphorylation and dephosphorylation activities (the CII half also possesses ATPase activity<sup>20</sup>) and facilitates interactions with the KaiA and KaiB proteins that entail conformational adjustments.<sup>16,35</sup>

Crystal structures of KaiC and its mutants have disclosed details of the surroundings of bound ATP in the CI and CII halves and the specific roles of individual amino acids. Glutamates E77 and E78 in the CI half and E318 and E319 in the CII half (Figure 1A) are in the proximity of ATP phosphates and are coordinated to Mg<sup>2+</sup> (Figure 2). E77 and E318 lie closer to the  $\gamma$ -phosphate group in the CI and CII halves than E78 and E319, respectively. The locations of the former render them the most likely candidates for the general base, either activating a water that then conducts the nucleophilic attack as the first step of hydrolysis (CI and CII halves) or abstracting the proton from T432 and S431 to initiate phosphorylation (E318 in CII). T432 is consistently positioned closer to E318 and  $\text{P}_\gamma$  in the crystal structures than S431, and these spatial constraints are likely at the origin of the observed order of phosphorylation.<sup>31</sup>

As shown in Figure 2, the phosphoryl transfers occur across the subunit interface; i.e., the  $\gamma$ -phosphate of ATP associated with subunit A (gray, Figures 1B and 2B) is transferred to T432 or S431 from subunit B (green, Figures 1B and 2B), with E318 (A subunit) proposed to act as the general base. Once phosphorylated, pT432 forms a salt bridge to R385 across the subunit interface (Figure 2B).<sup>29</sup> Because it is stabilized by a larger number of interactions between subunits, the nearly hyperphosphorylated form of KaiC observed in the crystal structure (six pT432 and four pS431 residues)<sup>28</sup> is expected to be more compact than the hypophosphorylated form. This is indeed borne out by small-angle X-ray scattering (SAXS) studies in solution that provided relative volumes for hexamers of KaiC mutants mimicking various phosphorylation states.<sup>36</sup> Interestingly, the residues corresponding to T432 and S431 in the CI half are E198 and E197, respectively, and CI residue A192 corresponds to the T426 phosphorylation site in CII

(Figures 1A and 2). Because we and others using different techniques (X-ray crystallography vs mass spectrometry)<sup>29,30</sup> did not identify any phosphorylation sites in CI and the T432E/S431E KaiC mutant does not exhibit phosphorylation at the two glutamates,<sup>31</sup> we conclude that nature's selection of the triad of E198, E197, and A192 in CI prevents a potential phosphoryl transfer in that half. Therefore, ATP hydrolysis in CI cannot be harnessed to the task of phosphorylation and apparently generates power for the enzymatic activities in CII.

The relatively long distances between the  $\gamma$ -phosphates of ATP molecules and phosphate groups on pT432 and pS431 residues in the crystal structures (>6 Å)<sup>31</sup> should not come as a surprise, because the conformation trapped in the crystal represents the product state of the kinase. The relatively low pH of  $\sim 5$  in the crystallization solution favors KaiC kinase activity.<sup>21</sup> Moreover, substitution of ATP by ATP $\gamma$ S prior to crystallization locks KaiC in the hyperphosphorylated state as thiophosphates are resistant to dephosphorylation (see, for example, the case of CaM kinase II).<sup>37</sup> Thus, the KaiC crystal structure likely also represents an inhibited form of the autophosphatase.

## ■ THE MECHANISM OF KAIC DEPHOSPHORYLATION REMAINS ENIGMATIC

Although we have gained a good understanding of the mechanisms of the ATPase and autokinase activities of KaiC and the order of phosphorylation, the KaiC autophosphatase activity appears to have attracted surprisingly little attention, and no detailed mechanism has been put forth in the literature.<sup>31</sup> As a result, the origins of the strict order of dephosphorylation, first pT432 and then pS431, remain obscure. Thus, it is possible that the kinase and phosphatase active sites colocalize, whereby particular residues, i.e., E318, may be involved in both activities. Alternatively, the switch from the hyper- to the hypophosphorylated form of KaiC could entail a relatively large conformational change at subunit interfaces and/or be coupled to KaiC subunit exchange.

KaiCII does not share conserved sequence motifs that are hallmarks of either the PPP or PPM families of protein serine/threonine phosphatases (PSPs).<sup>38</sup> Like many PPP and PPM family members, KaiC displays a dependence on  $Mg^{2+}$  [in terms of hexamerization (KaiC protein from *Synechococcus lividus* P2)<sup>39</sup> and activity (Figure 3)] and shares their

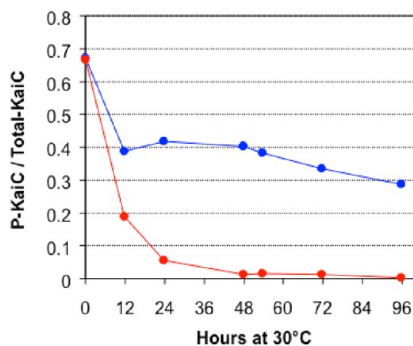


**Figure 3.**  $Mg^{2+}$  dependence of KaiC phosphatase activity. Dephosphorylation in the presence of 5 mM  $MgCl_2$  and 1 mM ATP (red curve). Dephosphorylation in a reaction buffer dialyzed (starting at time zero) against a solution containing 1 mM ATP but no  $MgCl_2$  (blue curve). We attribute the initial dephosphorylation activity indicated by the blue curve to the presence of residual  $Mg^{2+}$  despite dialysis.

multisubunit nature, but the concerted coupling of kinase and phosphatase at the subunit interfaces of a hexamer appears to be unique. The enzyme 6-phosphofructo-2-kinase/fructose-2,6-bisphosphatase combines kinase and phosphatase activities but does so by relying on distinct domains within a homodimer.<sup>40</sup> Certain PSPs are able to suppress the serine/threonine phosphatase in favor of a protein tyrosine phosphatase (PTP) and possess an ATPase that is apparently required for enhancing the tyrosine phosphatase activity.<sup>41,42</sup> However, we have not observed phosphorylation of Tyr residues in KaiC.

We hypothesized that the unique behavior of KaiC may be paired with an unusual mechanism of dephosphorylation, i.e., involving the regeneration of ATP from ADP in the CII half, thus bestowing an ATP synthase activity on KaiC and rendering the enzyme a phosphotransferase and not a phosphatase. In the presence or absence of the other two Kai proteins, the phases of KaiC kinase and ATPase cycles are similar and peak approximately 4 h before the hyperphosphorylated state is reached in a temperature-compensated manner.<sup>19</sup> Phosphorylation thus requires energy, and in the absence of incubation with ATP at 30 °C with or without KaiA, hyperphosphorylated KaiC spontaneously and slowly dephosphorylates. Structural studies of wild-type KaiC (wt-KaiC) and mutant KaiC proteins are consistent with a kinetic control of the order of phosphorylation<sup>31</sup> and the generation of a more compact,<sup>36</sup> albeit strained, higher-energy conformation. The KaiC hexamer flexing back to the relaxed form would then drive dephosphorylation, perhaps via a mechanism that produces ATP.

Here we survey published and new biochemical and structural data from our laboratories relevant to the dephosphorylation phase of the clock cycle and formulate a mechanism that generates ATP from ADP and pT432/pS431. KaiC is therefore a kinase, an ATPase, and an ATP synthase.

## EXPERIMENTAL PROCEDURES

**Protein Expression and Purification.** The *S. elongatus* KaiA, KaiB, and KaiC GST fusion proteins were expressed in *Escherichia coli* (BL21 cell line, Novagen/EMD Biochemicals) and purified following previously described protocols.<sup>27,30</sup> Site-directed mutagenesis of KaiC was performed by a modified method of Papworth et al.,<sup>43</sup> and GST fusions of all mutant proteins were expressed following the protocol used with wt-KaiC. Hexahistidine-tagged proteins were first purified by metal affinity chromatography (TALON IMAC resin, Takara Bio Clontech) and then by gel filtration chromatography (Sephacryl S-300 HR resin, GE Healthcare). GST fusion proteins were purified by affinity chromatography on glutathione-agarose resin (Pierce/Thermo Scientific) and cleaved from GST using human rhinovirus 3C protease. The proteins were further purified by ion exchange chromatography on Q-Sepharose with a gradient of NaCl. Wild-type and mutant proteins for crystallization were digested with trypsin and subsequently analyzed by matrix-assisted laser desorption/ionization time-of-flight mass spectrometry.

**$Mg^{2+}$  Dependence of Dephosphorylation.** A solution of 200 ng/ $\mu$ L KaiC was prepared in buffer containing 20 mM Tris-HCl (pH 8), 150 mM NaCl, 5 mM  $MgCl_2$ , 1 mM ATP, and 0.5 mM EDTA on ice. Dephosphorylation was assayed at 30 °C either in the presence of 5 mM  $MgCl_2$ , 0.5 mM EDTA, and 1 mM ATP or in a reaction buffer dialyzed against a solution containing 1 mM ATP and 0.5 mM EDTA but no  $MgCl_2$ . Neither reaction mixture contained KaiA or KaiB.

**Sodium Dodecyl Sulfate–Polyacrylamide Gel Electrophoresis (SDS–PAGE).** The phosphorylation states of the KaiC mutant proteins were assessed by SDS–PAGE. All proteins were expressed in *E. coli* and purified at 4 °C. Proteins were kept in 20 mM Tris-HCl (pH 8), 150 mM NaCl, 5 mM  $MgCl_2$ , 1 mM ATP, and 0.5 mM EDTA and were subjected to the following conditions prior to SDS–PAGE and Coomassie staining: (1) 200 ng/ $\mu$ L KaiC kept on ice for 24 h, (2) 200 ng/ $\mu$ L KaiC incubated at 30 °C for 24 h, (3) 200 ng/ $\mu$ L KaiC incubated with 50 ng/ $\mu$ L KaiA at 30 °C for 24 h, or (4) at 24 h, 1.35  $\mu$ L of 1.11  $\mu$ g/ $\mu$ L KaiB added to 10  $\mu$ L of reaction mixture 3 (final concentrations of the proteins being 176 ng/ $\mu$ L KaiC, 44 ng/ $\mu$ L KaiA, and 132 ng/ $\mu$ L KaiB) and then incubation at 30 °C continued for an additional 9 h.

**Crystal Structure of the KaiC E318A Mutant.** Protein expression, purification, and crystallization of the full-length, His<sub>6</sub>-tagged mutant protein were conducted following published protocols for wt-KaiC.<sup>28,39</sup> X-ray diffraction data were collected on the 21-ID-G beamline of the LS-CAT at the Advanced Photon Source (Argonne, IL) and processed with HKL2000.<sup>44</sup> Crystal data and data collection parameters are summarized in Table 1. Following structure determination by molecular replacement using the wt-KaiC coordinates [Protein Data Bank (PDB) entry 3DVL]<sup>12,13</sup> minus water as the search model, the structure was refined with PHENIX<sup>45</sup> using all data to 3.3 Å. Final refinement parameters are summarized in Table 1.

**Deposition of Crystallographic Data.** Final coordinates and structure factors for the crystallographic model of the *S. elongatus* KaiC E318A mutant protein have been deposited in the Protein Data Bank as entry 3UA2.

**KaiC ATP Synthase Activity Assay.** The reaction conditions were as follows: 180 ng/ $\mu$ L KaiC in 18 mM Tris-HCl, 135 mM NaCl, 4.5 mM  $MgCl_2$ , 0.45 mM EDTA, 0.45

**Table 1. Crystal Data and Refinement Statistics for the KaiC E318A Mutant**

Data Collection	
space group	<i>P</i> 2 <sub>1</sub> 2 <sub>1</sub> 2 <sub>1</sub>
unit cell constants (Å)	<i>a</i> = 131.71, <i>b</i> = 135.06, <i>c</i> = 204.25
X-ray source	APS, LS-CAT, 21-ID-G
detector	MAR300
wavelength (Å)	0.9872
resolution range (Å)	30–3.3 (3.42–3.30)
redundancy	8.4 (4.0)
<i>R</i> <sub>merge</sub> (%)	9.9 (42.6)
no. of unique reflections	42295 (2791)
completeness	91.3 (51.6)
<i>I</i> / $\sigma$ ( <i>I</i> )	10.5 (1.4)
Refinement	
<i>R</i> <sub>work</sub> (%)	23.0
<i>R</i> <sub>free</sub> (%)	30.7
no. of reflections used in <i>R</i> <sub>free</sub> (%)	5.0
overall average <i>B</i> factor (Å <sup>2</sup> )	98.3
no. of non-solvent atoms	24,097
no. of ATP molecules	12
no. of solvent molecules, Mg <sup>2+</sup> ions	67, 12
root-mean-square deviation from ideal geometry	
bonds (Å)	0.014
angles (deg)	1.1
Ramachandran plot (%)	
favored region	99.1
outliers	0.9

mM unlabeled ATP, and 2 nCi/ $\mu$ L ( $\approx$ 33  $\mu$ M) [8-<sup>14</sup>C]ADP (and 5% ethanol) (pH 8.0). The concentrations of unlabeled ADP and KaiA were 0.5 mM and 136 ng/ $\mu$ L, respectively. Nucleotides were separated by thin layer chromatography (TLC) on PEI-cellulose using 2 M HCOONa and then 4 M HCOONa (pH 3.4) as the developing solvent. TLC plates were developed for 80 min, dried, and exposed to a storage phosphor screen.

**RESULTS**

**Crystal Structure of KaiC E318A and Phosphorylation States of E319 Mutants.** Mutation of E318 that we postulate to be the general base in the CII kinase activity to alanine abolishes clock rhythmicity. However, the E318A mutant still retains a low level of phosphorylation according to analyses by either immunoblot with anti-KaiC antibodies<sup>31</sup> or SDS–PAGE (Figure 4A). Indeed, the newly determined crystal structure of the *S. elongatus* KaiC E318A mutant (Figure 4B) reveals that five of the six T432 residues still carry a phosphate group. However, in the structure of the E318A mutant protein, none of the S431 residues are phosphorylated (whereas in wt-KaiC six T432 and four S431 residues are phosphorylated). Thus, the crystallographic data indicate that phosphorylation of the E318A mutant is limited to a level that amounts to  $\sim$ 50% of wt-KaiC. With alanine in the KaiC E318A mutant itself unable to activate T432 and S431, the most probable candidates for mediating phosphorylation are E319 and Mg<sup>2+</sup> (Figure 2B). E319 is part of the outer coordination sphere of the divalent metal ion. The divalent metal ion might mediate phosphorylation via a coordinated hydroxyanion. To test these possibilities, we generated various E319 mutants and the E318/319A double mutant and assayed their phosphorylation

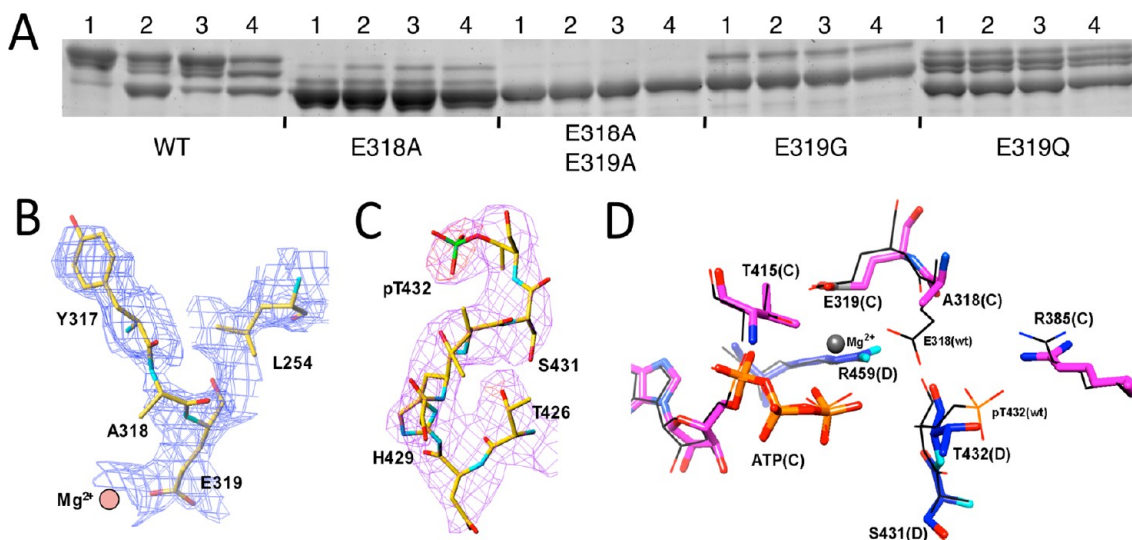


**Figure 4.** Phosphorylation states of KaiC E318A and several E319 mutants under various conditions and crystal structure of the *S. elongatus* KaiC E318A mutant. (A) wt-KaiC and E318/E319 mutants were expressed in *E. coli*, purified at 4 °C, and then subjected to the following conditions prior to SDS–PAGE and Coomassie staining (see Experimental Procedures for details). (1) KaiC was kept on ice for 24 h. (2) KaiC was incubated at 30 °C for 24 h. (3) KaiC was incubated with KaiA at 30 °C for 24 h. (4) At 24 h, KaiB was added to reaction mixture 3, and then the incubation at 30 °C was continued for an additional 9 h. (B) Quality of the KaiC E318A mutant crystal structure. Debaised omit electron density plotted at the 1 $\sigma$  level around A318 and E319 (both were omitted) at the A–B subunit interface. (C) Identification of phosphorylation at five T432 residues and the absence thereof at S431 residues in the KaiC E318A crystal structure. Fourier (*F*<sub>o</sub> – *F*<sub>c</sub>) difference electron density prior to incorporating phosphate into the model (3.5 $\sigma$  level, red) and final Fourier sum (2*F*<sub>o</sub> – *F*<sub>c</sub>) electron density (1 $\sigma$  level, magenta) in the region of pT432 (subunit A). (D) Superimposition of selected active site residues at the C–D subunit interface in the structures of E318A KaiC (thick bonds) and wt-KaiC (thin lines). In the E318A structure, subunit D is hypophosphorylated and carbon atoms of subunit C and D residues are colored magenta and blue, respectively. In the wt structure, subunit D is phosphorylated at T432 and carbon atoms are colored black.

states. The double mutant retains no kinase activity, and E319G is nearly hypophosphorylated (Figure 4A). E319D showed some phosphorylation (not shown), as did E318D that was arrhythmic.<sup>31</sup> By contrast, E319Q exhibits robust phosphorylation (Figure 4A), but this mutant is arrhythmic *in vivo*. Taken together, these data are consistent with a  $Mg^{2+}\cdots OH$ -mediated activation of threonine when E318 is not available. However, robust kinase activity requires both the catalytic glutamate and properly coordinated  $Mg^{2+}$  as demonstrated by the absence of phosphorylation in the E318/319A double mutant and the drastically reduced level of phosphorylation in the E319G mutant.

**Plasticity of the Subunit Interface.** A central question regarding dephosphorylation in KaiCII concerns the location of the site for this activity. Is the initiation of dephosphorylation preceded by a relatively large conformational change at the subunit interface, or is the transition more subtle, merely involving movements of a few angstroms? Crystal structures of wt-KaiC<sup>12,28</sup> and various mutants (ref 31 and this work) show similar overall conformations, devoid of large-scale changes in the conformations of residues in the vicinity of the ATP binding sites (<5 Å). Although we have not determined the structure of a hypophosphorylated form of KaiC, the crystal structure of the S431D mutant revealed phosphorylation of just three T432 residues.<sup>31</sup> In the crystal structure of the E318A mutant, subunit D is lacking phosphate on both T432 and S431. Comparison with the conformation of the corresponding subunit with T432 phosphorylated in the wt structure shows only minor movements of residues (Figure 4D). In the structure of the KaiC T432E/S431E double mutant, E432 residues display a position that differs from those of pT432 residues in the wt structure. Thus, the glutamates have moved away from R385 at the subunit interface and are now cradled by S379, S381, and T415 residues from the adjacent subunits.<sup>16</sup> Although the double-E mutant can be viewed as a mimic of the hyperphosphorylated form, it does not match the negative charge buildup of KaiC with 12 pT432 and pS431 residues. Overall, these crystallographic data support the notion of rather limited conformational flexibility in the vicinity of the phosphorylation sites, which is, however, clearly important for the proper function of the clock.<sup>35</sup>

It is possible that packing forces in crystals may oppose more significant conformational variations or that KaiCs with alternative conformational states of the CII ring may have resisted crystallization. However, the latter scenario is not supported by an analysis of the conformational variations of KaiC hexamers in solution. Thus, Murayama and co-workers used SAXS to analyze the overall shapes of wild-type and KaiC mutant proteins mimicking different phosphorylation states, *i.e.*, T432A/S431A, S431D, *etc.*<sup>36</sup> Their data are consistent with significant but relatively small changes in the overall volumes of these hexamers, and the observed maximal difference amounts to just 4%. Accordingly, the hyperphosphorylated state of KaiC is more compact than the hypophosphorylated state. This is consistent with the hyperphosphorylated state exhibiting interactions across the subunit interface (*i.e.*, pT432 $\cdots$ R385) and the formation of a hydrogen bond between pS431 and T426.<sup>28</sup> Our own investigations of KaiC molecules and Kai protein complexes using SAXS are not suggestive of substantial changes in the hexamer conformation either.<sup>16</sup> Thus, even if potentially sizable error margins in these measurements are taken into account, structural analyses of KaiCs in the solid state and in solution demonstrate that it is not necessary to

invoke a large-scale conformational change for KaiC to switch from phosphorylation to dephosphorylation.

**KaiC Subunit Exchange.** KaiC can undergo subunit exchange in the absence or presence of the two other Kai proteins.<sup>9,26,27</sup> Thus, KaiC hexamers alone appear to swap monomers, and when all three proteins are present, this process occurs predominantly during the dephosphorylation phase with KaiB bound to KaiC. Mathematical modeling of the KaiABC oscillator demonstrated that abolishing subunit exchange rapidly attenuates the amplitude, and it is thought that the exchange serves to maintain synchrony of the phosphorylation state among KaiC hexamers in the KaiC population as they oscillate over the *in vitro* cycle.<sup>27</sup> An experimental analysis subsequently showed by mixing hexamers at different phases of the oscillation that hexamers in the dephosphorylation phase could synchronize hexamers in other phases to the dephosphorylation phase.<sup>46</sup> At present, it is unclear how subunit exchange proceeds. However, EM micrographs of KaiC hexamers alone or in the presence of KaiA and/or KaiB have never revealed KaiC pentamers or heptamers.<sup>12,14,27,39</sup> It is important to keep in mind that KaiC can dephosphorylate by itself and therefore does not depend on KaiB for dephosphorylation. Moreover, phosphorylation and dephosphorylation require the hexameric state. Given the intricate interactions involving ATP,  $Mg^{2+}$ , and protein residues from adjacent CII domains, it is difficult to imagine how catalysis of dephosphorylation could proceed at the surface of a KaiCII subunit that is exposed because of the departure of the neighboring subunit. Although further research into the exchange process, *i.e.*, the role of particular mutations in potentially preventing or facilitating subunit exchange, is clearly warranted, it seems unnecessary to invoke such a dramatic event in trying to understand the mechanism of dephosphorylation. For now, we note that subunit exchange in the PTO may not be a prerequisite for dephosphorylation, but that it is more likely a consequence of KaiB binding and dephosphorylation of pT432.

#### Spacing of the Phosphatase and Kinase Active Sites.

As pointed out above, the KaiC sequence does not contain any of the various conserved motifs found in the three PSP families. Crystal structures offer other means of locating active sites, particularly when metal ion cofactors are involved. We have inspected electron density maps of KaiC crystal structures with resolutions of up to 2.6 Å but have not seen evidence of additional  $Mg^{2+}$  ions in CII domains.  $Mg^{2+}$  displays a strictly octahedral coordination geometry, and fully occupied binding sites can ordinarily be discerned even in low-resolution electron densities. There remains the possibility that potential metal ion coordination sites are not occupied without the phosphate substrates (pT432 and pS431) bound. Phosphorylated residues in CII engage in interactions with a range of residues, *i.e.*, R385 (pT432) and S379, S381, and T415 (with E432 in the structure of the KaiC T432E/S431E hyperphosphorylation mimic), *etc.* We will discuss the roles played by these residues in the next paragraph. Because the action of phosphatase (and ATPase) produces phosphate ions and the crystallization buffer can be supplemented with phosphate or sulfate, it is often possible to pinpoint the active site by locating anion(s) in crystal structures in the absence of signature sequences. We have been able to locate phosphate ions near the central channel of the hexamer in the KaiCI half of the KaiC A422V mutant structure (M. Egli and R. Pattanayek, unpublished data). However, we have not observed noncovalently bound phosphates in the CII half in

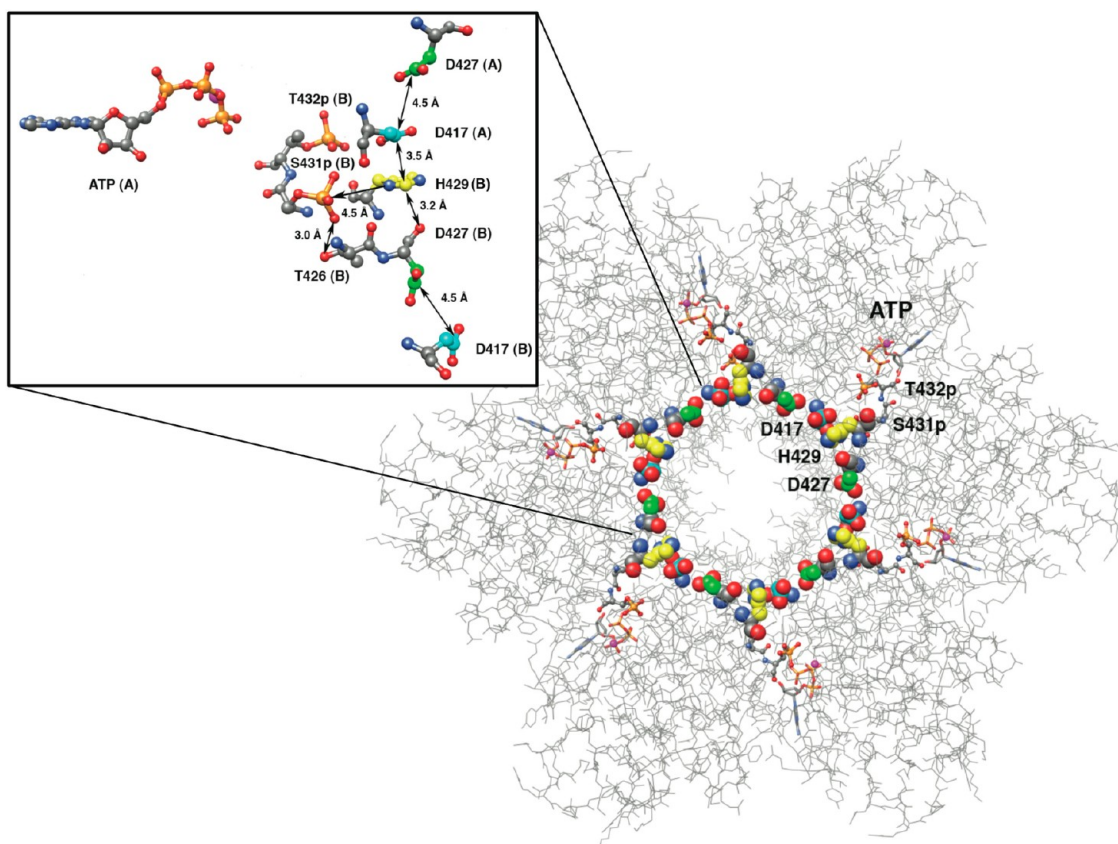


**Figure 5.** KaiCII half viewed from the CI side with side chain carbons of residues D417, H429, and D427 colored cyan, yellow, and green, respectively, to highlight the uninterrupted (DHD)<sub>6</sub> chain that encircles the central channel. The inset shows a close-up of a D417-H429-D427 triad at the subunit interface with its nearest neighbors. Individual subunits are labeled (A and B), and selected distances are shown in angstroms. Note the proximity of pS431 to T426 and H429.

any of the crystal structures determined to date. Therefore, bound cations or anions other than those near ATP molecules offer no insights into the location of the dephosphorylation activity at the subunit interface. Alternatively, the absence of such ions can be interpreted as evidence that phosphorylation and dephosphorylation occur at one and the same site.

**Functional Characterization of KaiC Mutations in the Vicinity of P-Sites.** We selected residues in the vicinity of pT432 and pS431 for a mutational screen to potentially gain insight into the seat and mechanism of dephosphorylation. The effects of individual mutations (typically Ala) on the clock period, phosphorylation profiles, and KaiC dephosphorylation over time were tested.<sup>31</sup> A first group of mutated residues located within or directly adjacent to the loop region harboring the pT432 and pS431 sites investigated in this fashion included H423A, H429A, D417A, D427A, D435A, and D435E. Histidines often participate in metal ion binding at active sites of phosphatases, serve as the general acid/base, or take on the role of the nucleophile as in phospholipase D (i.e., PLD-PMF).<sup>47</sup> Aspartates constitute key residues with phosphohydrolase members of the HAD superfamily, and the catalytic mechanism involves an aspartylphosphate intermediate.<sup>48</sup> Of course Asp and Glu also serve the coordination of metal ions at enzyme active sites (Figure 2).

We found that H423A and H429A exhibit phosphorylation patterns that are similar to that of wt-KaiC. The former mutant exhibits a nearly wt period of 23.3 h, whereas the latter features a slightly prolonged cycling time (27.5 h).<sup>31</sup> Interestingly, H429, D417, and D427 are engaged in a sandwich-like

interaction, whereby the two aspartates stack onto the His ring from opposite sides (Figure 5). In this way, six DHD triads encircle the central KaiCII channel seamlessly. This is a remarkable configuration because H429 is hydrogen bonded to pS431 in some subunits,<sup>13,29</sup> and DHD units could thus serve as relays for informing subunits of the phosphorylation states of their neighbors. Although this is an intriguing idea, D417A, like H429A, exhibits a phosphorylation pattern that resembles the wt profile and a period that is only slightly prolonged (25.6 h). On the other hand, D427A is arrhythmic as are D435A and D435E (D427E exhibits a long period, 29.8 h, at 30 °C in vivo). It is perhaps surprising that the mutation of D427 should trigger an effect so different from the effects of mutations of D417 and H429. However, D427 is a direct neighbor of T426 whose mutations all abolish rhythmicity (see the next paragraph). In addition to the intrasubunit contact to H429 via its carbonyl oxygen, the carboxylate moiety of the D427 residue is situated close to the side chains of S416 and S424. By comparison, the side chains of D435 and Q323 are hydrogen bonded across the subunit interface, and mutation of the former disrupts a contact that is apparently critical for KaiC stability and function and cannot be mimicked by a differently spaced carboxylate moiety (E435). Therefore, these residues may indirectly affect the courses of phosphorylation and/or dephosphorylation, but they are unlikely to be directly participating in the mechanism of the latter activity. It is possible that such residues are involved in the flexing of CII subunits entailing rhythmic compaction and expansion and/or the mediation of subunit exchange.<sup>16,35,36</sup>

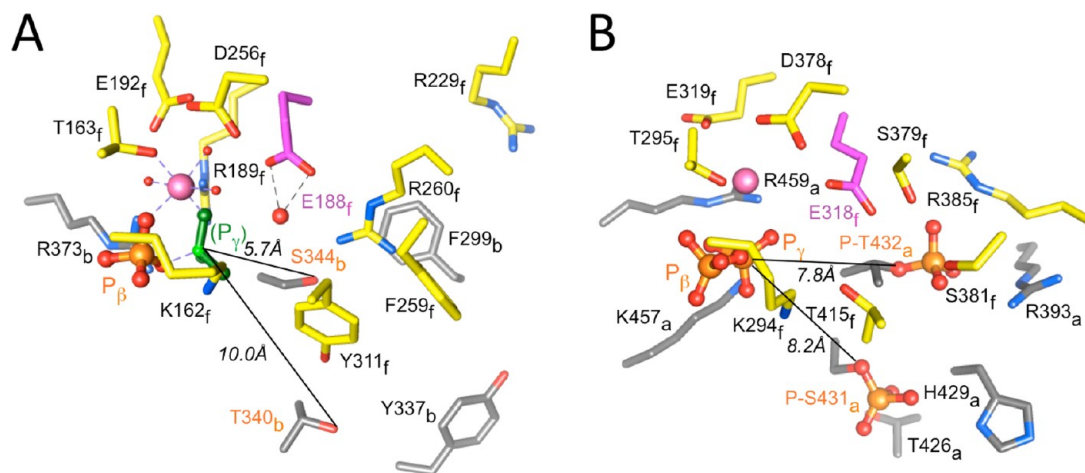


**Figure 6.** Striking similarities between the ATP binding sites at (A) the  $\alpha$ - $\beta$  heterodimer interface in F1-ATPase and (B) the subunit interface in KaiCII. The coordinates of F1-ATPase were taken from the crystal structure of the bovine enzyme inhibited by ADP and beryllium fluoride (PDB entry 1W0J).<sup>50</sup> The illustration for KaiCII in panel B is based on PDB entry 3DVL.<sup>12,28</sup> Carbon atoms of amino acid side chains in  $\alpha$  chain B of F1-ATPase and subunit A of KaiCII (see subscripts in labels) are colored gray. Carbon atoms of side chains in  $\beta$  chain F of F1-ATPase and subunit F of KaiCII are colored yellow. Only the  $\beta$ - and  $\gamma$ -phosphates of ATP are shown, whereby the latter is mimicked by  $\text{BF}_3$  (green) in the structure of F1-ATPase.  $\text{Mg}^{2+}$  ions are pink spheres with coordinated water molecules depicted as small red spheres in F1-ATPase (2.2 Å resolution). Carbon atoms of catalytic glutamates (E188 in F1 and E318 in CII) are highlighted with magenta carbons, and the water nucleophile (ATPase) hydrogen bonded to E188 in F1 is highlighted as a large red sphere.

A second group of residues tested with regard to their effects on phosphorylation pattern, clock period, and dephosphorylation behavior includes those that could reasonably be expected at an active site targeting phosphothreonine and phosphoserine and lie in the vicinity of the phosphorylation sites: R385, R393, S379, S381, and T415. The two serines and the threonine are hydrogen bonded across the subunit interface to E432 in the structure of the T432E/S431E double mutant.<sup>16</sup> Both R385 and R393 hover in the vicinity of pT432 (Figures 2B and 6B) and pS431,<sup>13,28</sup> although only the interactions with R385 are across the subunit interface. It is noteworthy that the E385A and E393A mutants have opposite effects on the phosphorylation pattern. R393A causes a shift to the hypophosphorylated form, whereas R385A boosts the hyperphosphorylation level.<sup>31</sup> We observed that R393A has a normal period, but that its oscillation is of low amplitude and that R385A features a long period of 36–48 h.<sup>31</sup> The dephosphorylation behavior of R385A resembles that of wt-KaiC, and we concluded that R385A may shift the equilibrium between the kinase and phosphatase activities in favor of the former rather than inhibit dephosphorylation.<sup>31</sup> Clearly, R385 is an interesting residue structurally and functionally. Its mutation to alanine results in a drastically distorted period without abolishing rhythmicity altogether, and while R385 appears to stabilize the kinase product state (Figure 2B), KaiC R385A still retains a high phosphorylation level. Only T415 was tested so far among residues S379, S381, and T415. Although its phosphorylation state is similar to that of the wt protein, the period is shortened to 19 h. To conclude, none of the assayed residues can be directly implicated in dephosphorylation, although R385 and T415 remain interesting on the basis of their proximity to phosphorylation sites and the observed changes upon mutation in the period (very long for R385A and short for T415A) and the altered phosphorylation state (R385A).

**Role of T426 in Dephosphorylation.** We reported earlier that the T426A mutation renders the clock arrhythmic<sup>29</sup> and that the residue at position 426 needs to be phosphorylatable

for proper clock function.<sup>31,32</sup> The observation that T426 was phosphorylated in the crystal structure of the KaiC T432E/S431A double mutant would support the idea that the phosphate is not simply swapped back and forth between S431 and T426. Rather, it seems to be transferred from ATP, most likely by the same mechanism established for phosphorylation of T432 and S431. However, T426 is even farther from the  $\gamma$ -phosphate (12 Å) than S431 (9 Å), and the greater distance may explain the smaller number of pT426 residues compared with the number of pT432 and pS431 residues in the crystal structures.<sup>31</sup> Spatial constraints within the phosphorylation loop prevent S431 and T426 from simultaneously carrying a phosphate group. In addition, T426 phosphorylation appears to be labile.<sup>32</sup>

With respect to the search for residues with a potential role in dephosphorylation, it is noteworthy that mutations of T426 affect the KaiC dephosphorylation kinetics. Thus, the arrhythmic T426N mutant significantly hinders the rate of dephosphorylation.<sup>32</sup> In addition, KaiB alone or mixtures of KaiA and KaiB added to the T426N or T426A KaiCs do not result in dephosphorylation as with wt KaiC, and these mutants thus remain locked in a permanently hyperphosphorylated state. Therefore, T426 is a primary candidate for a residue with a role in dephosphorylation that is situated in the immediate vicinity of pT432 and pS431 and adjacent to the kinase active site. Although the dephosphorylations of pT432 and pS431 likely proceed by the same mechanism, T426 may stabilize the latter via formation of a hydrogen bond,<sup>28</sup> thus determining the order of dephosphorylation. It is clear that the phosphate on T426 in the crystal structures of mutants could not have come from S431 as this residue was mutated to Ala in both cases.<sup>31</sup> However, we cannot exclude the alternative scenario in which a direct transfer of phosphate between S431 and T426 occurs in wt-KaiC. Such an exchange is consistent with everything we know about this residue: (i) the fact that T426 needs to be phosphorylatable for the clock to exhibit the proper period,<sup>31</sup> (ii) the prolonged presence of the pS431 band in SDS-PAGE gels tracking the *in vitro* KaiABC clock,<sup>34</sup> (iii) the resistance of

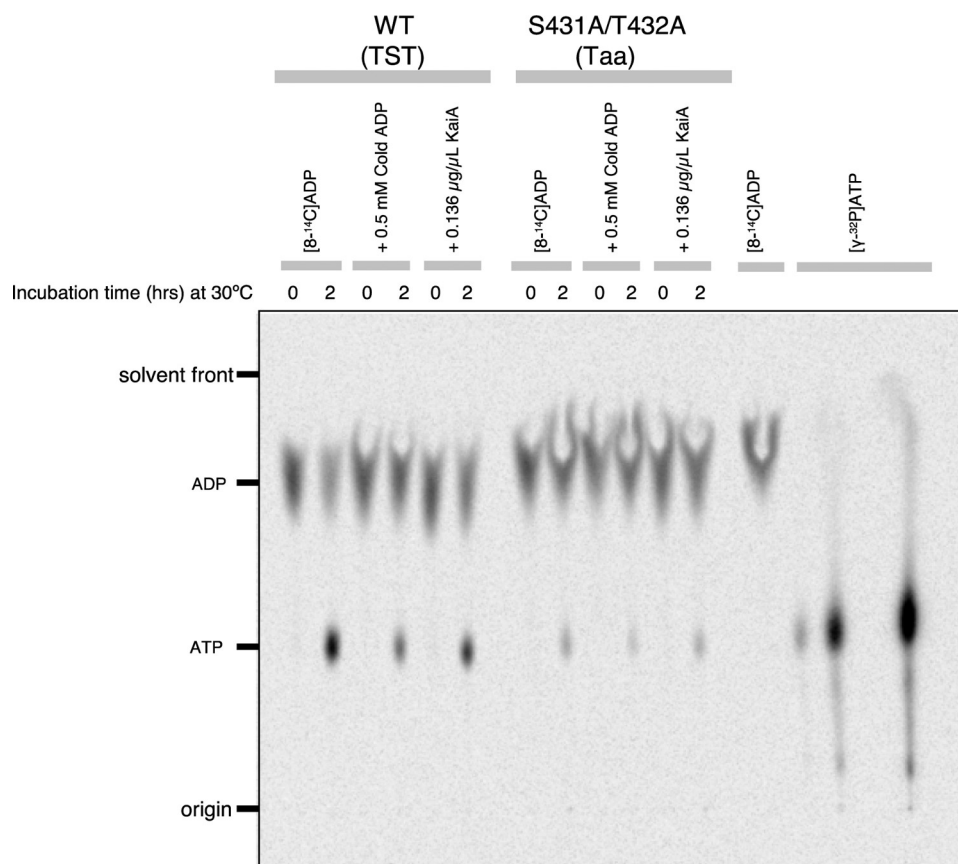


**Figure 7.** KaiC ATP synthase TLC activity assay (see Experimental Procedures for details).

T426 mutants to dephosphorylation,<sup>32</sup> and (iv) the high conformational rigidity of CII in the pS431 state.<sup>35</sup> Therefore, we propose that T426 is directly involved in dephosphorylation and argue that the active sites of kinase and phosphatase overlap at the KaiCII subunit interface. KaiC subunit exchange that sets in during its dephosphorylation and KaiB binding is unlikely to affect dephosphorylation of pS431 and its interaction with T426. Although more work is necessary to clarify this issue, subunit exchange may be promoted by dephosphorylation of pT432 that removes a salt bridge with R385 across the subunit interface (Figures 2B and 6B).

**Putative ATP Synthase Activity of KaiCII.** One possible reason for the difficulty in locating the phosphatase active site in KaiC might be that the enzyme uses an unusual mechanism to dephosphorylate T432 and S431. Thus, the ATPase and phosphatase activities in KaiC could somehow be linked such that the dephosphorylation reaction in KaiCII regenerates ATP, i.e., P-T432 + ADP → T432 + ATP, with KaiC thus possessing an ATP synthase activity and requiring us to reclassify it as a phosphotransferase. The energy required to convert ADP to ATP in CII could be produced in CI via the ATPase activity there, or it could stem from the ATPase activity at a different subunit interface in CII. In this context, it is worth remembering that the KaiCI and -II rings exhibit a close structural similarity to the trimer of  $\alpha$ - $\beta$  heterodimers in F1-ATPase.<sup>28</sup> This close similarity extends to the interfaces between  $\alpha$  and  $\beta$  chains [F1 (Figure 6A)] and between KaiC subunits [illustrated for KaiCII (Figure 6B)]. Moreover, it is known that CaM kinase-II converts ADP to ATP by reversing the kinase reaction and removing the phosphate from the previously phosphorylated T286.<sup>37</sup> Unlike KaiC, CaM kinase-II

does not possess an ATPase activity to generate energy to potentially convert ADP to ATP. Instead, a conformational change may account for the required input in energy needed to catalyze the reaction.

We tested the hypothesis of KaiC synthesizing ATP by using <sup>14</sup>C-labeled ADP and assaying the potential formation of ATP by thin layer chromatography. Initial experiments were supportive of a significant ADP → ATP activity from a preparation of wild-type KaiC that was 95% pure (Figure 7). Interestingly, the KaiC T432A/S431A double mutant also displayed an activity that corresponds to ~10–20% of that for wt-KaiC. The latter observation seems to contradict an ATP synthase mechanism of dephosphorylation as the double mutant is not expected to be able to adopt the hyperphosphorylated state and subsequently hand back phosphate to bound ADP. However, we know that KaiCII also possesses ATPase activity.<sup>20</sup> In fact, the ATPase activities of the T432A/S431A mutant either in the context of full-length KaiC or of a separate KaiCII hexamer are substantially higher than the ATPase activity of wt-KaiC.<sup>20</sup> To explain the ATP synthase activity of KaiC T432A/S431A, we hypothesize that KaiCII can hand back to ADP either orthophosphate (reversal of the ATPase) or phosphate attached to T432 and S431, thus forming ATP. However, formation of ATP by dephosphorylation of pT432 and pS431 in wt-KaiC is enhanced compared to formation of ATP from ADP and P<sub>i</sub> in the double mutant that favors the ATPase activity. An open question concerns the amount of energy required to drive dephosphorylation and thus ATP synthesis and how ATPase activity is partitioned between the KaiCI and KaiCII halves.

## ■ NEW CONCEPT FOR THE MECHANISM OF KAI C DEPHOSPHORYLATION

There is no evidence from structural studies using either crystallography or SAXS that the switch from the KaiC phosphorylation to the dephosphorylation phase involves a significant conformational change at the subunit interface or that the phosphatase active site is situated in the interior of CII domains rather than between subunits. Dephosphorylation requires  $Mg^{2+}$  (Figure 3), but besides the ions associated with ATP, no additional ions were found in electron density maps. Moreover, no obvious coordination sites, i.e., clusters of Asp/Glu residues, are present in the three-dimensional structure. The crystal structure and the results from site-directed mutagenesis point to E77 and E318 acting as the general base in the CI (ATPase) and CII (kinase) halves, respectively (Figure 2). Residues whose mutation strongly affects KaiC phosphorylation levels include R385 (R385A displays a very long period and exhibits enhanced kinase activity) and T426 (T426A, T426N, and T426E are all arrhythmic and exhibit delayed dephosphorylation).<sup>31,32</sup> Both residues map to the immediate vicinity of the pT432 and pS431 phosphorylation sites, thus providing support for overlapping kinase and phosphatase active sites. Other residues that are near pT432 and pS431 and display a distorted period or arrhythmic behavior upon mutation to alanine include T415 (forms a hydrogen bond to E432 in the structure of the T432E/S341E hyperphosphorylation mimic) and D427 (mediates subunit interactions near the central channel). However, mutation of H423 and H429 that are also close to the phosphorylation sites had only a minor effect on the period or phosphorylation pattern and therefore are unlikely to play a catalytic role.

After more than a decade of attributing KaiC dephosphorylation to a phosphatase activity, we now have gathered the first evidence that KaiC is actually a phosphotransferase that hands back the phosphates on T432 and S431 to ADP, making it effectively an ATP synthase (Figure 8). Although we cannot at the moment exclude the possibility, it is unlikely that pT432 and pS431 proceed with different mechanisms, i.e., via ATP synthesis in the case of T432 and via hydrolysis in the case of S431. The environments of phosphothreonine 432 and phosphoserine 431 at the KaiCII subunit interface are quite different (Figures 2B and 6B). Therefore, the order of dephosphorylation, pT432 first and pS431 second, is most likely not a consequence of different mechanisms but is due to the shorter distance between pT432 and  $P\beta$  of ADP relative to the corresponding distance for pS431. Another factor that might delay the transfer of the phospho group from pS431 is its intrasubunit interaction with T426 (Figures 2B and 6B). Because CII, like CI, is an ATPase, that reverse reaction likely also proceeds via an ATP synthase mechanism. This is supported by the detection of ATP in the assay with the KaiC T432A/S431A mutant (Figure 7).

The discovery of the KaiC ATP synthase activity and similarities between the F1-ATPase ( $\alpha\beta$ )<sub>3</sub> and KaiCII<sub>6</sub> (as well as KaiCI<sub>6</sub>) structures at the global<sup>28</sup> and subunit interface levels (Figure 6) help clarify the roles of individual active site residues in the catalysis of the various reactions. The most likely interpretation of the accumulated observations is that E318 constitutes the general base for both kinase and ATPase in CII. Thus, incubation with ATP drives ATPase activity in CI and provides the energy to phosphorylate T432 and S431 in CII. In the kinase mode, E318 deprotonates first T432 and then S431,

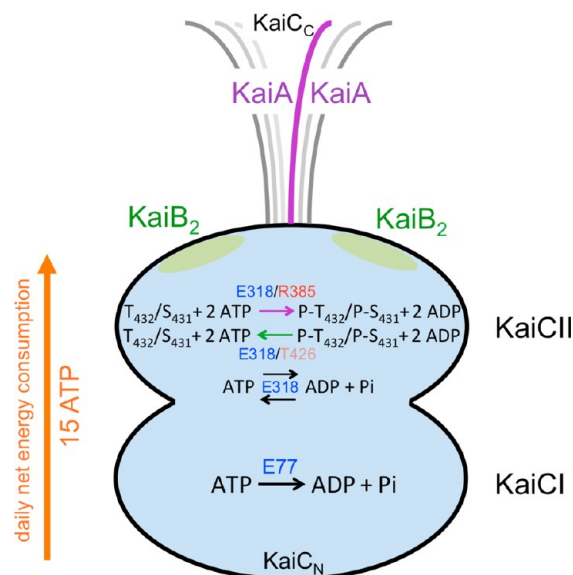


**Figure 8.** Schematic of the KaiABC PTO with the reactions catalyzed in the KaiCI and KaiCII halves. Only the CII half harbors phosphorylation (kinase) and dephosphorylation (phosphotransferase = ATP synthase) activities. Both CI and CII are ATPases, and the reverse reaction also results in ATP. The net energy consumed per day amounts to 15 ATPs,<sup>19</sup> but the absolute numbers of ATP molecules hydrolyzed and synthesized over the daily cycle are unknown.

whereby nucleophile generation is kinetically controlled. Phosphorylation locks KaiC in a strained and more rigid higher-energy form that involves formation of salt bridges between pT432 and R385 residues across subunit interfaces and formation of hydrogen bonds between pS431 and T426 (Figures 2B and 6B). In the absence of the further input of energy from ATP hydrolysis, KaiCII switches to the dephosphorylation mode, presumably driven by a subtle conformational change back to the initial conformation, which is more relaxed and less compact.

Dephosphorylation also involves E318, but now glutamic acid first cradles the phosphate moiety of pT432 and later that of pS431 and, aided by  $Mg^{2+}$  and R459 (Figure 6B), delivers the phosphates back to ADP. This mechanism is the same as in the case of F1-ATPase [E188 and R189 (Figure 6A)],<sup>51</sup> except that F1 uses orthophosphate as the substrate instead of phosphothreonine and phosphoserine. However, CII also catalyzes the  $ADP + P_i \rightarrow ATP$  reaction (Figures 7 and 8). It is noteworthy in this respect that the E318A mutant resists dephosphorylation even in the presence of KaiB compared with wt-KaiC (Figure 4A, WT and E318A, lanes 4), thus implicating E318 in the dephosphorylation reaction. The order of dephosphorylation is probably determined by the relative proximity of phosphorylated residues to the general base to some degree, as well. However, T426 also plays an important role, by stabilizing pS431 and thereby prolonging its lifetime, and possibly undergoing phosphoryl transfer and subsequently mediating dephosphorylation. In analogy to the role of E188 in ATP hydrolysis catalyzed by F1-ATPase (Figure 6A), E318 can be expected to generate the hydroxide ion that then conducts the nucleophilic attack at the  $\gamma$ -phosphate.

Two of the most fascinating properties of the KaiABC circadian clock are the long period and the unexpectedly small consumption of energy (15 ATP molecules per day<sup>19</sup>). In light of our postulate of an ATP synthase mechanism of

dephosphorylation, it is clear that we do not know the absolute number of ATP molecules hydrolyzed during the daily cycle. Thus, the ATP synthase activity may serve as an ATP conservation mechanism to reduce the total number of ATP molecules hydrolyzed, so that the clock can run accurately in vivo even under nonoptimal metabolic conditions when the cellular ATP levels may be low. The KaiC ATPase activity is obviously of fundamental importance for clock function, and we can speculate that the KaiCII phosphorylation and dephosphorylation cycle that exhibits a period of ~24 h serves to regulate the activity of the ATPase that is also compensated by temperature.<sup>19</sup> Currently, we have a very limited understanding of the mechanism of transfer of energy between the KaiCI and KaiCII halves and potential allosteric effects in the control of the chemical reactions that occur at the subunit interfaces. We would expect the CII kinase activity and ring compaction to be fueled by ATP hydrolysis in CI. Whether the conformational change back to the relaxed form is sufficient to drive dephosphorylation or if additional input of ATPase from CI and/or CII is needed is an open question. Further, it is unclear whether CI exhibits ATP synthase activity as well and, if so, at which phase during the 24 h cycle ATP synthesis there occurs. Gaining insight into these and undoubtedly other questions will be the goal of future research. Even in the absence of firm answers, the similarities between two evolutionarily ancient molecular machines, one generating cellular energy and the other measuring time by using energy seemingly very sparingly, are highly intriguing.

## AUTHOR INFORMATION

### Corresponding Author

\*Department of Biochemistry, Vanderbilt University, School of Medicine, 607 Light Hall, Nashville, TN 37232-0146. Telephone: (615) 343-8070. Fax: (615) 322-7122. E-mail: martin.egli@vanderbilt.edu.

### Funding

We are grateful to the National Institutes of Health for supporting clock research in our laboratories (Grant R01 GM073845 to M.E. and Grant R01 GM067152 to C.H.J.). Use of the Advanced Photon Source (APS) was supported by the U.S. Department of Energy, Office of Science, Office of Basic Energy Sciences, under Contract DE-AC02-06CH11357. Use of LS-CAT Sector 21 was supported by the Michigan Economic Development Corp. and the Michigan Technology Tri-Corridor for the support of this research program (Grant 08SP1000817). The DuPont-Northwestern-Dow Collaborative Access Team (DND-CAT) Synchrotron Research Center at sector 5 of the APS was supported by E. I. DuPont de Nemours & Co., The Dow Chemical Company, the National Science Foundation, and the State of Illinois.

## ACKNOWLEDGMENTS

We thank Dr. Spencer Anderson, LS-CAT, APS, Argonne National Laboratory (Argonne, IL), for help with X-ray data collection and Prof. Roger J. Colbran (Vanderbilt University, School of Medicine) for insightful discussions regarding mechanistic aspects of phosphatases. We thank an anonymous reviewer of a previously published paper on the KaiABC clock for drawing our attention to the possibility of an ATP synthase mechanism. Our hypothesis and experimental evidence that the dephosphorylation of KaiC proceeds via ATP synthesis is also

supported by unpublished data from Nishiwaki et al. (Nagoya University), which will be published separately.

## REFERENCES

- (1) Dunlap, J. C., Loros, J. J., and DeCoursey, P. J. (2004) *Chronobiology: Biological Timekeeping*, Sinauer, Sunderland, MA.
- (2) Johnson, C. H. (2004) Precise circadian clocks in prokaryotic cyanobacteria. *Curr. Issues Mol. Biol.* 6, 103–110.
- (3) Ditty, J. L., Mackey, S. R., and Johnson, C. H., Eds. (2009) *Bacterial Circadian Programs*, Springer Publishers Inc., Heidelberg, Germany.
- (4) Ishiura, M., Kutsuna, S., Aoki, S., Iwasaki, H., Andersson, C. R., Tanabe, A., Golden, S. S., Johnson, C. H., and Kondo, T. (1998) Expression of a gene cluster *kaiABC* as a circadian feedback process in cyanobacteria. *Science* 281, 1519–1523.
- (5) Xu, Y., Mori, T., and Johnson, C. H. (2000) Circadian clock-protein expression in cyanobacteria: Rhythms and phase setting. *EMBO J.* 19, 3349–3357.
- (6) Tomita, J., Nakajima, M., Kondo, T., and Iwasaki, H. (2005) Circadian rhythm of KaiC phosphorylation without transcription-translation feedback. *Science* 307, 251–254.
- (7) Nakajima, M., Imai, K., Ito, H., Nishiwaki, T., Murayama, Y., Iwasaki, H., Oyama, T., and Kondo, T. (2005) Reconstitution of circadian oscillation of cyanobacterial KaiC phosphorylation in vitro. *Science* 308, 414–415.
- (8) Qin, X., Byrne, M., Yu, X., Mori, T., and Johnson, C. H. (2010) Coupling of a core post-translational pacemaker to a slave transcription/translation feedback loop in a circadian system. *PLoS Biol.* 8, e1000394.
- (9) Johnson, C. H., Stewart, P. L., and Egli, M. (2011) The cyanobacterial circadian system: From biophysics to bioevolution. *Annu. Rev. Biophys.* 40, 143–167.
- (10) Iwasaki, H., Taniguchi, Y., Kondo, T., and Ishiura, M. (1999) Physical interactions among circadian clock proteins, KaiA, KaiB and KaiC, in cyanobacteria. *EMBO J.* 18, 1137–1145.
- (11) Taniguchi, Y., Yamaguchi, A., Hijikata, A., Iwasaki, H., Kamagata, K., Ishiura, M., Go, M., and Kondo, T. (2001) Two KaiA-binding domains of cyanobacterial circadian clock protein KaiC. *FEBS Lett.* 496, 86–90.
- (12) Pattanayek, R., Williams, D. R., Pattanayek, S., Xu, Y., Mori, T., Johnson, C. H., Stewart, P. L., and Egli, M. (2006) Analysis of KaiA-KaiC protein interactions in the cyanobacterial circadian clock using hybrid structural methods. *EMBO J.* 25, 2017–2038.
- (13) Johnson, C. H., Egli, M., and Stewart, P. L. (2008) Structural insights into a circadian oscillator. *Science* 322, 697–701.
- (14) Pattanayek, R., Williams, D. R., Pattanayek, S., Mori, T., Johnson, C. H., Stewart, P. L., and Egli, M. (2008) Structural model of the circadian clock KaiB-KaiC complex and mechanism for modulation of KaiC phosphorylation. *EMBO J.* 27, 1767–1778.
- (15) Egli, M., and Stewart, P. L. (2009) Structural aspects of the cyanobacterial KaiABC circadian clock. In *Bacterial Circadian Programs* (Ditty, J. L., Mackey, S. R., and Johnson, C. H., Eds.) pp 121–140, Springer Publishers Inc., Heidelberg, Germany.
- (16) Pattanayek, R., Williams, D. R., Rossi, G., Weigand, S., Mori, T., Johnson, C. H., Stewart, P. L., and Egli, M. (2011) Combined SAXS/EM based models of the *S. elongatus* posttranslational oscillator and its interactions with the output His-kinase Sasa. *PLoS One* 6, e23697.
- (17) Kageyama, H., Kondo, T., and Iwasaki, H. (2003) Circadian formation of clock protein complexes by KaiA, KaiB, KaiC, and Sasa in cyanobacteria. *J. Biol. Chem.* 278, 2388–2395.
- (18) Leippe, D. D., Aravind, L., Grishin, N. V., and Koonin, E. V. (2000) The bacterial replicative helicase DnaB evolved from a RecA duplication. *Genome Res.* 10, 5–16.
- (19) Terauchi, K., Kitayama, Y., Nishiwaki, T., Miwa, K., Murayama, Y., Oyama, T., and Kondo, T. (2007) The ATPase activity of KaiC determines the basic timing for circadian clock of cyanobacteria. *Proc. Natl. Acad. Sci. U.S.A.* 104, 16377–16381.
- (20) Murakami, R., Miyake, A., Iwase, R., Hayashi, F., Uzumaki, T., and Ishiura, M. (2008) ATPase activity and its temperature

compensation of the cyanobacterial clock protein KaiC. *Genes Cells* 13, 387–395.

(21) Nishiwaki, T., Iwasaki, H., Ishiura, M., and Kondo, T. (2000) Nucleotide binding and autophosphorylation of the clock protein KaiC as a circadian timing process of cyanobacteria. *Proc. Natl. Acad. Sci. U.S.A.* 97, 495–499.

(22) Iwasaki, H., Nishiwaki, T., Kitayama, Y., Nakajima, M., and Kondo, T. (2002) KaiA-stimulated KaiC phosphorylation in circadian timing loops in cyanobacteria. *Proc. Natl. Acad. Sci. U.S.A.* 99, 15788–15793.

(23) Xu, Y., Mori, T., and Johnson, C. H. (2003) Cyanobacterial circadian clockwork: Roles of KaiA, KaiB, and the *kaiBC* promoter in regulating KaiC. *EMBO J.* 22, 2117–2126.

(24) Williams, S. B., Vakonakis, I., Golden, S. S., and LiWang, A. C. (2002) Structure and function from the circadian clock protein KaiA of *Synechococcus elongatus*: A potential clock input mechanism. *Proc. Natl. Acad. Sci. U.S.A.* 99, 15357–15362.

(25) Kitayama, Y., Iwasaki, H., Nishiwaki, T., and Kondo, T. (2003) KaiB functions as an attenuator of KaiC phosphorylation in the cyanobacterial circadian clock system. *EMBO J.* 22, 1–8.

(26) Kageyama, H., Nishiwaki, T., Nakajima, M., Iwasaki, H., Oyama, T., and Kondo, T. (2006) Cyanobacterial circadian pacemaker: Kai protein complex dynamics in the KaiC phosphorylation cycle in vitro. *Mol. Cell* 23, 161–171.

(27) Mori, T., Williams, D. R., Byrn, M., Qin, X., Egli, M., Mchaourab, H., Stewart, P. L., and Johnson, C. H. (2007) Elucidating the ticking of an in vitro circadian clockwork. *PLoS Biol.* 5, e93.

(28) Pattanayek, R., Wang, J., Mori, T., Xu, Y., Johnson, C. H., and Egli, M. (2004) Visualizing a circadian clock protein: Crystal structure of KaiC and functional insights. *Mol. Cell* 15, 375–388.

(29) Xu, Y., Mori, T., Pattanayek, R., Pattanayek, S., Egli, M., and Johnson, C. H. (2004) Identification of key phosphorylation sites in the circadian clock protein KaiC by crystallographic and mutagenetic analyses. *Proc. Natl. Acad. Sci. U.S.A.* 101, 13933–13938.

(30) Nishiwaki, T., Satomi, Y., Nakajima, M., Lee, C., Kiyohara, R., Kageyama, H., Kitayama, Y., Temamoto, M., Yamaguchi, A., Hijikata, A., Go, M., Iwasaki, H., Takao, T., and Kondo, T. (2004) Role of KaiC phosphorylation in the circadian clock system of *Synechococcus elongatus* PCC 7942. *Proc. Natl. Acad. Sci. U.S.A.* 101, 13927–13932.

(31) Pattanayek, R., Mori, T., Xu, Y., Pattanayek, S., Johnson, C. H., and Egli, M. (2009) Structures of KaiC circadian clock mutant proteins: A new phosphorylation site at T426 and mechanisms of kinase, ATPase and phosphatase. *PLoS One* 4, e7529.

(32) Xu, Y., Mori, T., Qin, X., Yan, H., Egli, M., and Johnson, C. H. (2009) Intramolecular regulation of phosphorylation status of the circadian clock protein KaiC. *PLoS One* 4, e7509.

(33) Nishiwaki, T., Satomi, Y., Kitayama, Y., Terauchi, K., Kiyohara, R., Takao, T., and Kondo, T. (2007) A sequential program of dual phosphorylation of KaiC as a basis for circadian rhythm in cyanobacteria. *EMBO J.* 26, 4029–4037.

(34) Rust, M. J., Markson, J. S., Lane, W. S., Fisher, D. S., and O'Shea, E. K. (2007) Ordered phosphorylation governs oscillation of a three-protein circadian clock. *Science* 318, 809–812.

(35) Chang, Y., Kuo, N., Tseng, R., and LiWang, A. (2011) Flexibility of the C-terminal, or CII, ring of KaiC governs the rhythm of the circadian clock of cyanobacteria. *Proc. Natl. Acad. Sci. U.S.A.* 108, 14431–14436.

(36) Murayama, Y., Mukaiyama, A., Imai, K., Onoue, Y., Tsunoda, A., Nohara, A., Ishida, T., Maéda, Y., Terauchi, K., Kondo, T., and Akiyama, S. (2011) Tracking and visualizing the circadian ticking of the cyanobacterial clock protein KaiC in solution. *EMBO J.* 30, 68–78.

(37) Kim, S. A., Hudmon, A., Volmer, A., and Waxham, M. N. (2001) CaM-kinase II dephosphorylates Thr286 by a reversal of the autophosphorylation reaction. *Biochem. Biophys. Res. Commun.* 282, 773–780.

(38) Shi, Y. (2009) Serine/threonine phosphatases: Mechanism through structure. *Cell* 139, 468–484.

(39) Mori, T., Saveliev, S. V., Xu, Y., Stafford, W. F., Cox, M. M., Inman, R. B., and Johnson, C. H. (2002) Circadian clock protein KaiC

forms ATP-dependent hexameric rings and binds DNA. *Proc. Natl. Acad. Sci. U.S.A.* 99, 17203–17208.

(40) Hasemann, C. A., Istvan, E. S., Uyeda, K., and Deisenhofer, J. (1996) The crystal structure of the bifunctional enzyme 6-phosphofructo-2-kinase/fructose-2,6-bisphosphatase reveals distinct domain homologies. *Structure* 4, 1017–1029.

(41) Cayla, X., Goris, J., Hermann, J., Hendrix, P., Ozon, R., and Merlevede, W. (1990) Isolation and characterization of a tyrosyl phosphatase activator from rabbit skeletal muscle and *Xenopus laevis* oocytes. *Biochemistry* 29, 633–642.

(42) Chao, Y., Xing, Y., Chen, Y., Xu, Y., Lin, Z., Li, Z., Jeffrey, P. D., Stock, J. B., and Shi, Y. (2006) Structure and mechanism of the phosphotyrosyl phosphatase activator. *Mol. Cell* 23, 535–546.

(43) Papworth, C., Bauer, J. C., Braman, J., and Wright, D. A. (1996) Site-directed mutagenesis using double-stranded plasmid DNA templates. *Strategies* 9, 3–4.

(44) Otwinowski, Z., and Minor, W. (1997) Processing of X-ray diffraction data collected in oscillation mode. *Methods Enzymol.* 276, 307–326.

(45) Adams, P. D., Afonine, P. V., Bunkóczi, G., Chen, V. B., Davis, I. W., Echols, N., Headd, J. J., Hung, L.-W., Kapral, G. J., Grosse-Kunstleve, R. W., McCoy, A. J., Moriarty, N. W., Oeffner, R., Read, R. J., Richardson, J. S., Terwilliger, T. C., and Zwart, P. H. (2010) PHENIX: a comprehensive Python-based system for macromolecular structure solution. *Acta Crystallogr. D* 66, 213–221.

(46) Ito, H., Kageyama, H., Mutsuda, M., Nakajima, M., Oyama, T., and Kondo, T. (2007) Autonomous synchronization of the circadian KaiC phosphorylation rhythm. *Nat. Struct. Mol. Biol.* 14, 1084–1088.

(47) Leiros, I., McSweeney, S., and Hough, E. (2004) The reaction mechanism of phospholipase D from *Streptomyces* sp. strain PMF. Snapshots along the reaction pathway reveal a pentacoordinate reaction intermediate and an unexpected final product. *J. Mol. Biol.* 339, 805–820.

(48) Lu, Z., Dunaway-Mariano, D., and Allen, K. N. (2008) The catalytic scaffold of the haloalkanoic acid dehalogenase enzyme superfamily acts as a mold for the trigonal bipyramidal transition state. *Proc. Natl. Acad. Sci. U.S.A.* 105, 5687–5692.

(49) Vakonakis, I., and LiWang, A. C. (2004) Structure of the C-terminal domain of the clock protein KaiA in complex with a KaiC-derived peptide: Implications for KaiC regulation. *Proc. Natl. Acad. Sci. U.S.A.* 101, 10925–10930.

(50) Kagawa, R., Montgomery, G., Braig, K., Walker, J. E., and Leslie, A. G. W. (2004) The structure of bovine F<sub>1</sub>-ATPase inhibited by ADP and beryllium fluoride. *EMBO J.* 23, 2734–2744.

(51) Blanchet, M. A., Hüllihen, J., Pedersen, P. L., and Amzel, L. M. (1998) The 2.8-Å structure of rat liver F<sub>1</sub>-ATPase: Configuration of a critical intermediate in ATP synthesis/hydrolysis. *Proc. Natl. Acad. Sci. U.S.A.* 95, 11065–11070.